

Article

Self-Lubricating Properties of Polyether-Ether-Ketone Composites Filled with CNTs@RC2540 Nano-Capsules

Jiju Guan ^{1,*} , Zhengya Xu ¹, Lei Zheng ¹, Lanyu Yang ¹ and Shuiquan Huang ^{2,*} 

¹ College of Mechanical Engineering, Changshu Institute of Technology, Suzhou 215500, China; zhuzb@cslg.edu.cn (Z.X.); alei611@163.com (L.Z.); yly@cslg.edu.cn (L.Y.)

² School of Mechanical Engineering, Yanshan University, Qinhuangdao 066000, China

* Correspondence: dawejiju@163.com (J.G.); shuiquan.huang@ysu.edu.cn (S.H.)

Abstract: Polyether-ether-ketone (PEEK) exhibits great potential in being a replacement for metal components across various applications relying on the mechanical and tribological properties. However, there is still much to be done to improve its properties. The main motivation of this paper is to improve the tribological and mechanical properties of PEEK simultaneously for more severe working environment. Therefore, dialkyl pentasulfide (RC2540) was proposed to fill into the cavity of CNTs to prepare nano-capsules, which were then filled into PEEK to prepare PEEK/nano-capsules composites. The existence of nano-capsules in PEEK was analyzed, and the friction and wear properties exhibited by PEEK composites against GCr15 steel were examined using pin-disk friction pairs, and the self-lubricating mechanism of PEEK composites in friction was revealed. Findings of this study indicated that when the mass fraction of nano-capsules was less than 5%, the filling of nano-capsules could improve the tensile strength of PEEK and reduced the friction coefficient and specific wear rate of PEEK by filling nano-capsules. During the friction process, RC2540 in the nano-capsules can be released as PEEK wears so that a self-lubricating layer can be formed for reducing PEEK composites' friction and wear.

Keywords: carbon nanotubes; nano-capsules; PEEK composites; self-lubrication



Citation: Guan, J.; Xu, Z.; Zheng, L.; Yang, L.; Huang, S. Self-Lubricating Properties of Polyether-Ether-Ketone Composites Filled with CNTs@RC2540 Nano-Capsules. *Lubricants* **2023**, *11*, 511. <https://doi.org/10.3390/lubricants11120511>

Received: 16 October 2023
Revised: 17 November 2023
Accepted: 30 November 2023
Published: 1 December 2023



Copyright: © 2023 by the authors. Licensee MDPI, Basel, Switzerland. This article is an open access article distributed under the terms and conditions of the Creative Commons Attribution (CC BY) license (<https://creativecommons.org/licenses/by/4.0/>).

1. Introduction

Polyether-ether-ketone (PEEK) is a commonly used polymer material with a low coefficient of friction and good thermal stability. It is increasingly applied in aerospace, automobile manufacturing, electronic and electrical, and healthcare fields, finding itself in an irreplaceable role in many fields. When it comes to mechanical application, PEEK is often used to manufacture bearings, insulation, seals and other components [1–3]. When PEEK is used as the material of pure water components such as pumps and valves, severe wear often occurs when it rubs against steel under water lubrication, especially at higher speeds and loads. This is due to the high coefficient of linear expansion and poor creep resistance of pure PEEK. Therefore, graphite, MoS₂, carbon fiber and glass fiber are often applied to modify it to meet the requirements of use. Literature reviews [4–7], on the effect of SiO₂, ZrO₂, Si₃N₄, SiC and other nanoparticles on PEEK composites' friction and wear properties (tribological properties) have shown that the coefficient of friction (COF) of the material decreases with the increase in nanoparticles content. The composites showed the lowest COFs when the content of SiO₂, ZrO₂ and Si₃N₄ was about 15%. As the content of nanoparticles increased, the wear front decreased and then rose. The COF decreased with the increase in loadings, which indicated that the COF could be more obviously impacted by nanoparticles under higher loadings. M. Zalaznik and Moskalewicz [8,9] investigated the influence of filling content of MoS₂ on PEEK materials' mechanical and tribological properties. The results indicate that PEEK composites showed the optimal tribological properties when the MoS₂ content was 5%, with a 25% and 20% reduction in the COF and

wear rate (WR), respectively, as compared to pure PEEK. The reason why MoS₂ improves PEEK composites' tribological properties is that the friction process is accompanied by the formation of a transfer film on the friction substrate surface.

Carbon nanotubes (CNTs) have favorable mechanical characteristics, such as tensile strengths that can reach 200 GPa, making them an ideal reinforcement phase for PEEK. Studies [10,11] show that CNTs with high hardness and fibrosis can be wound more tightly into the PEEK system during curing to enhance the PEEK's mechanical properties. In addition, the friction property of PEEK/CNT composites is also better than that of pure PEEK. This is because the exfoliated CNTs can be distributed at the friction interface as a third body, isolating the rough contact between the lubrication system and acting as a certain role of self-lubrication [12]. Kalin [13] investigates the effect of surface untreated CNTs and graphene powder on PEEK tribological properties. It was found that 2 wt.% CNTs significantly reduced the COF but increased the WR. However, graphene was incapable of improving the tribological properties of PEEK, which may be closely related to the surface treatment of CNTs and graphene. Song [14] studied the friction and wear properties exhibited by PEEK composite coatings filled with oxidized graphene and acidified CNTs. The results demonstrated that adding a few acidified CNTs or oxidized graphene could remarkably lower the composites' COF and enhance the wear resistance. The PEEK/graphene composites exhibited better anti-friction and wear resistance than the PEEK/CNT composites, suggesting that the surface modification has a great influence on the antifriction and wear resistance of nanometer fillers.

CNTs have a special cavity structure with an inner diameter of between 5 and 50 nm. Under certain conditions, the introduction of other liquid substances into the cavities of CNTs can improve the self-conductive properties, magnetic properties and friction properties, etc. [15–18]. To prepare CNT nano-capsules, we proposed to fill the cavities of CNTs with various lubricants in the study. This filling method can introduce more lubricants into the molecules of CNTs and improve its lubrication properties. If nano-capsules are used as a filler for polymers such as PEEK, the lubricant in CNTs can be protected during the curing process so that the PEEK composites material contain liquid lubricant. During friction, the nano-capsules in PEEK composites can release the lubricant, which can effectively improve PEEK composites' tribological properties. Moreover, nano-capsules can be better dispersed in the PEEK for enhancing the composites' mechanical properties.

In this paper, the lubricant RC2540 (dialkyl pentasulfide) was applied to the preparation of CNTs@RC2540 nano-capsules, and the nano-capsules were used to prepare PEEK composites. How the filling of the nano-capsules impacted PEEK composites' mechanical and tribological properties in comparison with normal CNTs was investigated, and the releasing and self-lubricating mechanism of RC2540 in the process of friction was analyzed. This leads to an increase in the mechanical strength of PEEK and further improvement in its tribological properties. Unlike the research results in the published works above, this study found that after filling the nano-capsules with PEEK, it can not only increase its strength, but also better improve its tribological properties using liquid lubricants. This study lays the foundation for the formula selection and preparation process of this new PEEK composites material used in self-lubricating moving parts.

2. Materials and Methods

2.1. Preparation of CNTs@RC2540 Nano-Capsules

Multi-walled carbon nanotubes (MWCNTs) of 99% purity and 20–50 nm inner diameter were provided by Shanghai Aladdin Biochemical Technology (Shanghai, China). The CNTs purchased had a large aspect ratio of about 1000:1, which was not conducive for filling. Therefore, the CNTs were first pretreated for short duration. A mixture of 50 g of CNTs and 1500 mL of 40% concentrated nitric acid was loaded into a three-mouth flask to receive 8 h of reflux treatment at 80 °C, followed by magnetic stirring at 500 r/min. After

vacuum filtering, the obtained filter cake underwent drying treatment at 85 °C and 10 h of ball milling and acidified CNTs were obtained at last.

The liquid-phase wet chemical method was used to prepare nano-capsules [19,20]. 10 g of RC2540 was dissolved in 400 mL of acetone, added with 20 g of acidified CNTs. After the complete mixing, the mixture was packed into a spherical flask, followed by being vacuumized to -0.1 MPa pressure. Under this condition, the mixture was ultrasonic stirred for 2 h at 65 °C. Then, the mixture was filtered under vacuum condition and washed in acetone to remove the unfilled RC2540. Finally, the filter cake underwent 12 h of drying treatment in an oven at 75 °C, and ball milling was applied to obtain CNTs@RC2540 nano-capsules. Figure 1 displays the preparation process of CNTs@RC2540 nano-capsules.

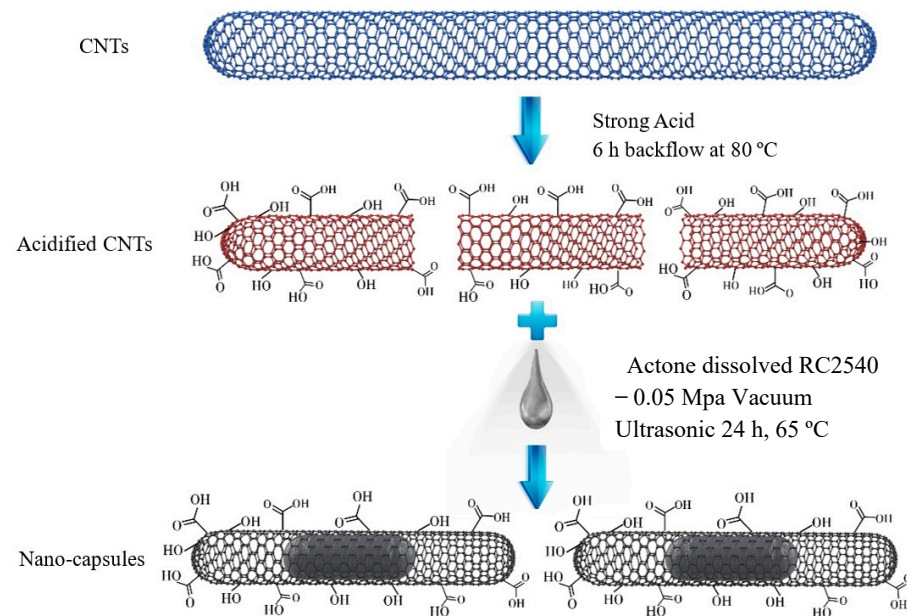


Figure 1. Schematic illustration for the preparation process of CNTs@RC2540 nano-capsules.

A Nicolet 6700 infrared spectrometer was adopted to detect the Fourier transform infrared (FTIR) spectrometry of RC2540, acidified CNTs and the nano-capsules. A FEI TECNAI G20 transmission electron microscope (TEM) detected specimen' microstructure at an acceleration voltage of 200 KV [21,22]. Thermogravimetric analysis of CNTs and nano-capsules was conducted using an STA449 thermal analyzer with a temperature range of 20–800 °C and a rise rate of 20 °C/min, and the atmosphere was N₂ with a flow rate of 40 mL/min [23].

2.2. Preparation of PEEK Composites

150XF PEEK powder was purchased from VICTREX Plc. Acidified CNTs and CNTs@RC2540 nano-capsules were added into PEEK powder at levels ranging from 1% to 9%, respectively. After thorough mechanical mixing, the mixture powder was ball-milled for 8 h and then the mixture was poured into an “Eight-Shaped” cavity mold and a “Ring-Shaped” cavity mold, respectively. Cold-pressing technology was adopted to pressure the powder into a Φ 40 mm \times 10 mm “Eight-Shaped” block specimen and Φ 30 mm \times 12 mm ring specimen under the molding pressure of 30 MPa, respectively. After pressing, the specimens were placed in a programmable oven for curing, as shown in Figure 2a. The specimens were cured under the following conditions [24]: curing temperature: 343 °C; and temperature rise rate: 10 °C/h. After natural cooling, the specimens were finally prepared. The eight-shaped block specimens were used for a mechanical property test, and the ring specimens were used for friction test after being cut into pin specimen.

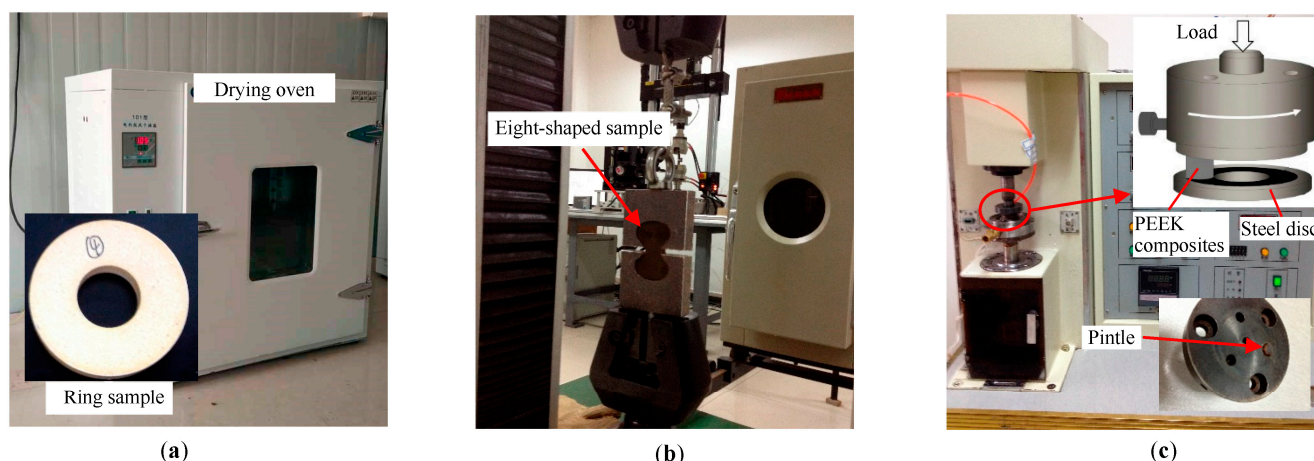


Figure 2. The experimental process of this article: preparation of samples (a), tensile test (b) and tribological test (c).

2.3. Mechanical and Friction Properties Tests

The tensile strength of the eight-shaped block was tested using an RG 4100 universal material testing machine (Figure 2b) according to ISO standards. The tensile rate was 1 mm/min, and the deformation curve breaking strength of PEEK and its composites were automatically recorded by the testing machine [25,26]. The specimen hardness was tested by an HR-150A Rockwell hardness tester with Φ 12.7 mm diameter of indenter with a main load of 588 N and a pre-load of 98 N in the hardness test (HRR). The hardness values were measured at four locations (three points at each location) and then averaged.

According to the ASTM standards, we conducted friction tests on the MMW-1 friction and wear testing machine (Figure 2c), and Table 1 lists the basic experimental conditions. The COF is calculated as:

$$\mu = T/(Pr) \quad (1)$$

where T is friction torque, P is test loading, r is radius of the contact point trajectory and is about 11.25 mm. The COF is taken as the average value in the test period. The mass of the pin specimen before and after tests was weighed. In the calculation formula of the specific wear rate:

$$W = \Delta V/(Pd) \quad (2)$$

where ΔV is the wear volume, and d is the sliding distance and can be calculated by test time, rotation radius r and rotation speed. The experimental protocol is as follows:

- The influence of filler content on the PEEK composites' tribological properties was tested at a test load of 50 N and a sliding speed of 0.5 m/s. At this stage, the filler content varied from 1 wt.% to 10 wt.%.
- The influence of sliding speed on the tribological properties exhibited by 5 wt.% nanoparticles-filling PEEK was tested at a test load of 50 N. In this test, the sliding speed was changed from 0.1 m/s to 0.9 m/s.
- The influence of test load on the tribological properties exhibited by 5 wt.% nanoparticles-filling PEEK was investigated at a sliding speed of 0.5 m/s. In this test, the load was changed from 20 N to 80 N.

Table 1. Friction and wear test conditions.

Test Equipment	Friction Pair	Pin	Disc	Lubrication Condition	Test Temperature	Test Time	Repeated Experiments
MMW-1 friction testing machine	Pin on disc	PEEK composites, Diameter: Φ 4 mm, Length: 12 mm,	GCr15 steel ring, Ra: 0.2 μ m. Outside diameter: Φ 30 mm, Inside diameter: φ 15 mm, Hardness: 59–61 HRC,	Water lubrication, flow rate of 0.5 L/min	25 °C	10 min	3 times

2.4. Surface Analysis

The FTIR spectra of PEEK and nano-capsules were measured before and after curing using a Nicolet 6700 infrared spectrometer [27]. The microstructure of PEEK composites was observed using a SIRION-100 FESEM. The worn disks were removed under a test load of 50 N and a sliding speed of 0.5 m/s and cleaned with acetone under ultrasound for 30 min, which corresponds to a filler content of 5% in the PEEK composite. An AXIS Ultra DLD X-ray photoelectron spectroscope (XPS) helped to analyze the binding energy of the main elements on the worn surface. The electron pass energy was 80 eV, the ray source was monochromatic AlK α , and a binding energy of 284.8 eV for adventitious carbon C_{1s} was taken as the internal standard. SEM also served for observing the worn surface microstructure of PEEK composites.

3. Experimental Results

3.1. Characterization of CNTs@RC2540 Nano-Capsules

Figure 3 displays the results of thermogravimetric (TG) and differential scanning calorimetry (DSC) of RC2540, ordinary CNTs and nano-capsules. As indicated in Figure 3a, the TG curve of normal CNTs changes gently under low temperature, while the TG curve of nano-capsule has a significant weight loss process at about 295 °C, which is the result of RC2540 escaping from the nano-capsules under the condition of heat. This also demonstrates the presence of RC2540 in the CNTs. Equation (3) explains the calculation of the filling rate (η) of RC2540 in CNTs [28–30].

$$\eta = H_f / H_p \times 100\% \quad (3)$$

where H_f denotes the phase-transition latent heat of RC2540-filled CNTs, and J/g and H_p refers to that of RC2540 at the same quality. As for the DSC curve of the nano-capsules in Figure 3b, the calculated result of the phase transition latent heat of RC2540 is 29.5 J/g (A1: Area enclosed by the DSC curve and baseline), while that of RC2540 under the same conditions is 121.3 J/g (A2: Area enclosed by the DSC curve and baseline). Hence, we confirmed the filling rate of RC2540 in CNTs as 24.3%.

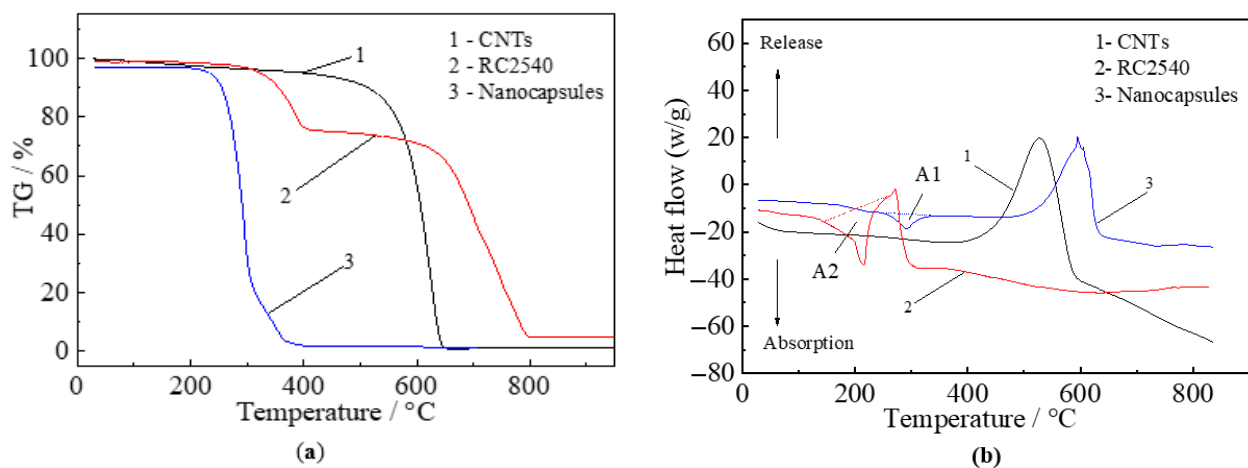


Figure 3. Thermogravimetric analysis of CNTs, RC2540 and nano-capsules: TG (a), DSC (b).

Figure 4 shows the FTIR spectra of acidified CNTs, RC2540 and CNTs@RC2540 nano-capsules. It can be seen from Figure 4a that the new absorption peaks of CNTs around 3432 cm⁻¹ and 1822 cm⁻¹ wavelengths after acidification treatment are a result of hydroxyl and carboxyl groups [31], revealing the binding of acidified CNTs to oxygen-containing groups, that is good for improving the bonding strength of CNTs and PEEK during curing. Furthermore, the peak near 1643 cm⁻¹ is a result of the plane absorption peak of the carbon ring structure [32,33]. That is to say, CNTs preserve tubular structures, which is the

prerequisite for the CNTs to be filled with RC2540. It can be found from Figure 4a that the FTIR spectrum of nano-capsules does not present any new characteristic peaks, and the characteristic peaks are partial superimpositions of these of the acidified CNTs and RC2540, indicating that in the process of filling CNTs with RC2540, physical combination mainly occurs between them, but no chemical reaction. By observing the microstructure of carbon tubes with TEM, the state of RC2540 in CNTs tubes can be visually determined. Figure 4b shows a TEM of the nano-capsules. Several sections of the tubes were clearly infiltrated with RC2540, which visually demonstrates the presence of RC2540 in the CNTs tubes.

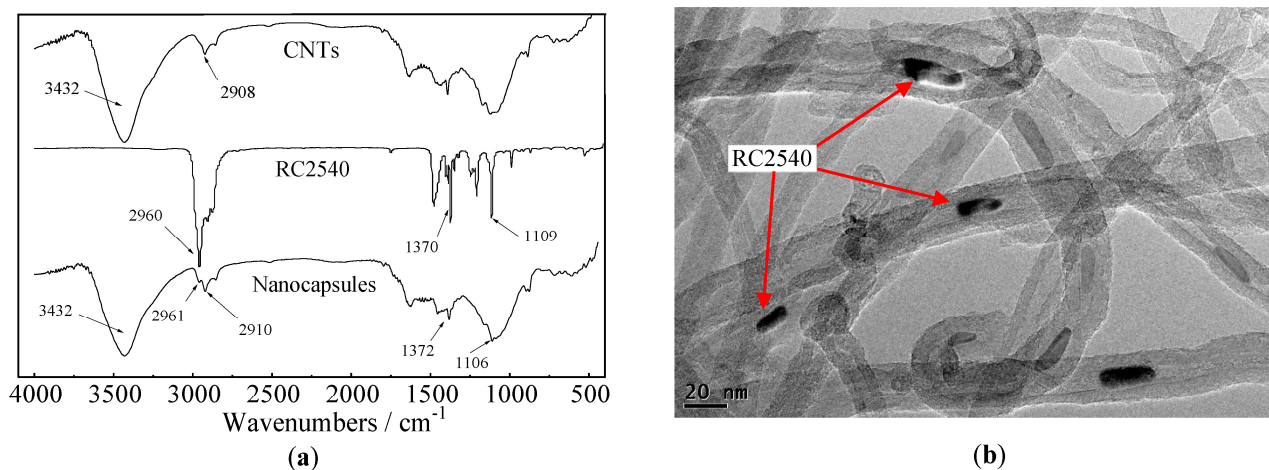


Figure 4. Structural characterization of nano-capsule: FTIR (a) spectrum and TEM (b).

3.2. Mechanical Property and Interior Structure of PEEK Composites

Figure 5 indicates how the mass fractions of CNTs and nano-capsules affect the PEEK composites' tensile strength and hardness. In Figure 5a, with the increase in the filling amount, the tensile strength presents an increase-to-decrease trend. Because CNTs show higher surface activity and many unsaturated bonds and reactive groups are formed [34]. The reinforced bond of PEEK can be strengthened by physical or chemical crosslinking of polymer chain and CNTs [35–37]. Further addition may lead to problems with the aggregation of CNTs, thereby reducing this cross-linking effect as well as reducing the PEEK composite strength. CNTs have an optimum content of about 5%, and the strength of PEEK can be increased by about 35% at this point, which is better than the method of filling CNTs in most of the literature reports above. At a filling level of approximately 8%, the strength of the PEEK composite is comparable to that of pure PEEK. The filling of nano-capsules more remarkably impacts PEEK strength and hardness because the nano-capsules have a smaller aspect ratio and are more closely bound to PEEK. Figure 5b suggests that the PEEK composite hardness decreases as the filling amount elevates. In practice, the appropriate filling amount can be selected according to the requirements of different self-lubricating parts [38].

Due to the complexity of the PEEK curing reaction, CNTs@RC2540 nano-capsules can possibly be destroyed in the curing process, so the stability of nano-capsules in the curing process and its compatibility with PEEK shall be studied. According to the TG curves of CNTs and nano-capsules in Figure 3, the nano-capsules show no significant weight loss until 300 °C, making them strong enough to deal with the curing temperature of PEEK. Figure 6a displays the FTIR spectra of PEEK, nano-capsules and the PEFE composites powder. The peaks of 1112 cm^{-1} , 1635 cm^{-1} , 2924 cm^{-1} and 3424 cm^{-1} in the nano-capsules spectrum, respectively, represent the absorption peaks of carbon nanotube skeleton vibration, C-H stretching vibration, C-H deformation vibration and O-H bond stretching vibration [39]. Among them, the first three peaks clearly appeared in the FTIR spectrum of the cured PEEK. That is to say, the CNTs' skeleton structure was not destroyed in the curing process, which can well protect the RC2540 within it. Figure 6b shows the SEM images of PEEK

composites tissue. Nano-capsules are distributed in the PEEK organization in the form of lump-like particles [40]. Each particle is an oil-containing nano-capsules that is destroyed during friction, while RC2540 is uniformly released for lubrication in the process of friction.

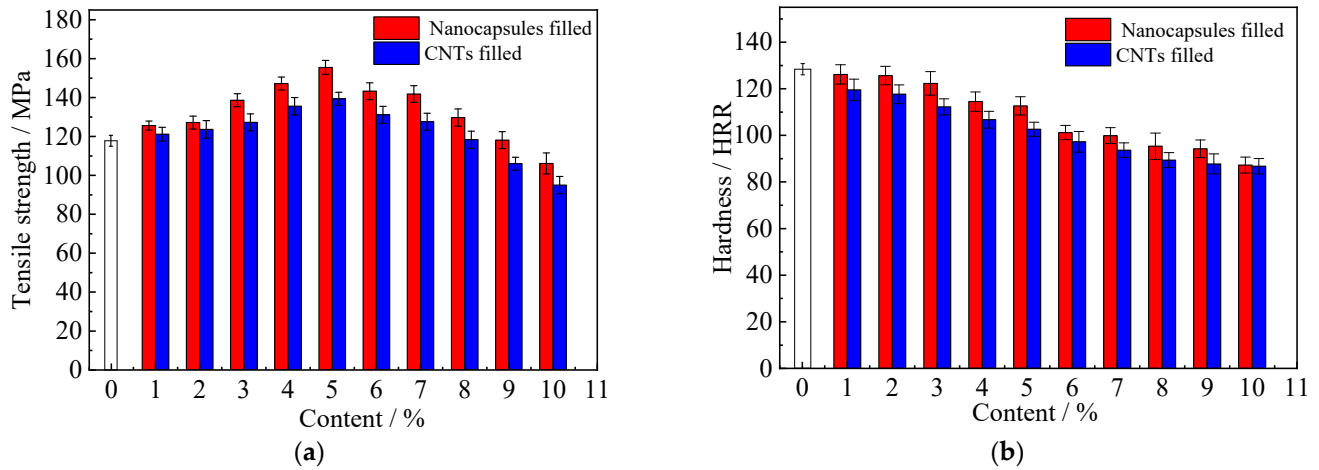


Figure 5. Effect of filler content on tensile strength (a) and hardness (b) of PEEK composites.

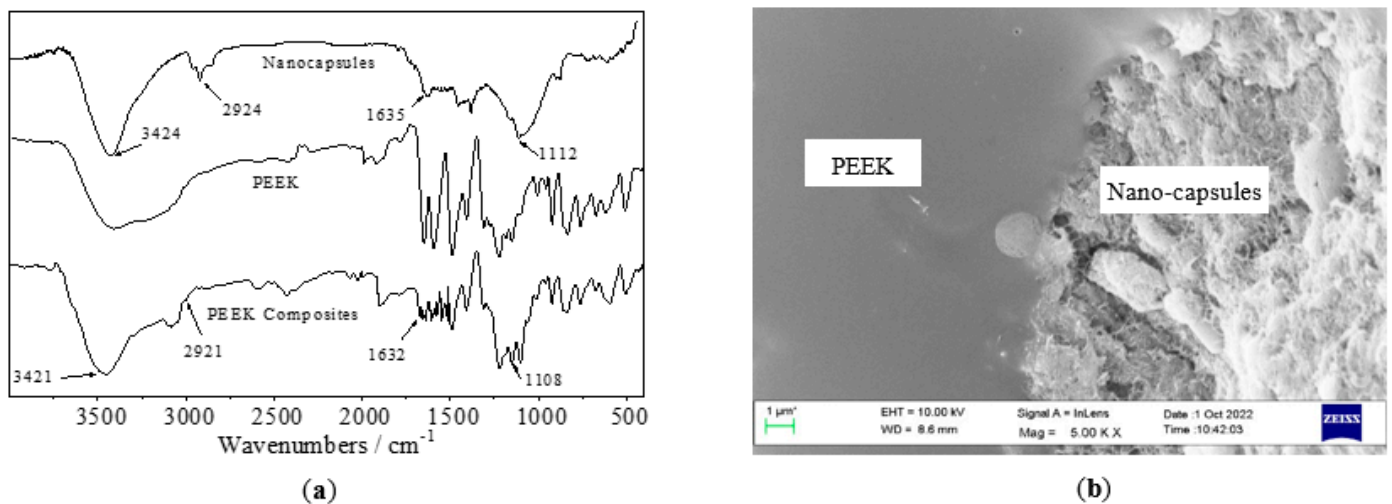


Figure 6. Characterization of structure: FTIR spectra of PEEK and composite (a), SEM image of composites (b).

3.3. Effect of Filling Content on PEEK Composites' Tribological Properties

Figure 7 shows the influence of the filling content of CNTs or nano-capsules on the COF and WR of PEEK at a load of 50 N and a sliding speed of 0.5 m/s. In Figure 7a, the lower content of CNTs leads to a certain diminution of the COF of PEEK, which is due to the molecular structure of the CNTs being destroyed during friction, and the adsorption and sedimentation of the CNT' molecular fragments may produce certain an anti-friction effect [41]. Then, the CNTs content exceeded 4% and continued to rise, the anti-friction effect of PEEK/CNTs became less significant, as excess CNTs might act as a deterrent. When filling with nano-capsules, the COF of PEEK/nano-capsule composite decreased with the increase in the content. It can be found that during friction, RC2540 was released from the nano-capsule inside PEEK, and RC2540 was adsorbed on the friction interface, which formed a more adequate lubrication and thus served to reduce the friction [42,43]. In Figure 7b, the WR is highest for pure PEEK. A transfer film can be formed at the friction interface of PEEK, that is not very strongly bonded to the metal. Filling CNTs or nano-capsules reduces the WR of PEEK, with minimum WRs of $2.7 \times 10^{-6} \text{ mm}^3/\text{N}\cdot\text{m}$ and

$1.9 \times 10^{-6} \text{ mm}^3 \text{ N}\cdot\text{m}$ at 15% or 10% filling, respectively. The value of this wear rate and the friction coefficient values mentioned above are superior to all relevant literature reports above. The adsorption and deposition of CNTs molecular fragment produced anti-friction effect on the friction interface, but also prevented a PEEK transfer film from being formed to some extent, reducing the WR of composites. The increasing amount of filler affects the hardness of composites [44], resulting in increased WR. The PEEK/nano-capsule composite had a lower WR than the PEEK composites under various contents. The WR result also shows that RC2540 is released during friction, and that the lubrication layer composed of RC2540 is more resistant to the adhesion and transfer of PEEK and therefore more effective against wear.

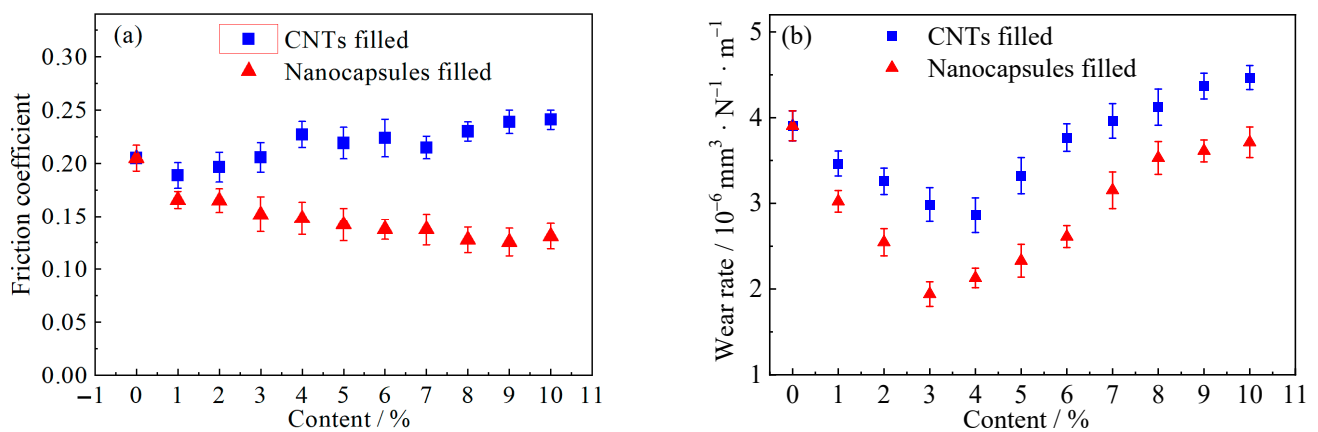


Figure 7. Effect of content on friction coefficient (a) and wear rate (b) of PEEK composites.

3.4. Effect of Sliding Speed on PEEK Composites' Tribological Properties

Figure 8 displays the effect of sliding speed on the COF and WR of pure PEEK, PEEK/CNT composite and PEEK/nano-capsule composite materials under a 50 N test load at a 5% filling of CNTs or nano-capsules. The COFs of the three materials have a decreasing tendency with the increase in sliding speed, which is mainly related to the temperature change, deformation, roughness and vibration between contact surfaces caused by the increasing speed [45,46]. In Figure 8a, PEEK/CNT composite has a smaller COF than pure PEEK under various velocities, with the PEEK/nano-capsule composite having the lowest coefficient of friction. The WR of the three materials increases with the increase in the speed in Figure 8b, and the PEEK/nano-capsule composite has the lowest WR. The high speed leads to an increase in temperature between the friction interfaces, which is more favorable to the release of RC2540 in the PEEK/nano-capsule composite material. The formation of a more adequate lubrication layer, as a result, leads to a significant downward trend in the COF of PEEK/nano-capsule composites. The linear velocity of high-speed machine parts when velocity can be above 40 m/s [47]. Under such conditions, the sliding between friction interfaces should be more conducive for the cleavage of nano-capsules, which promote RC2540 to be released and the self-lubrication layer to be formed.

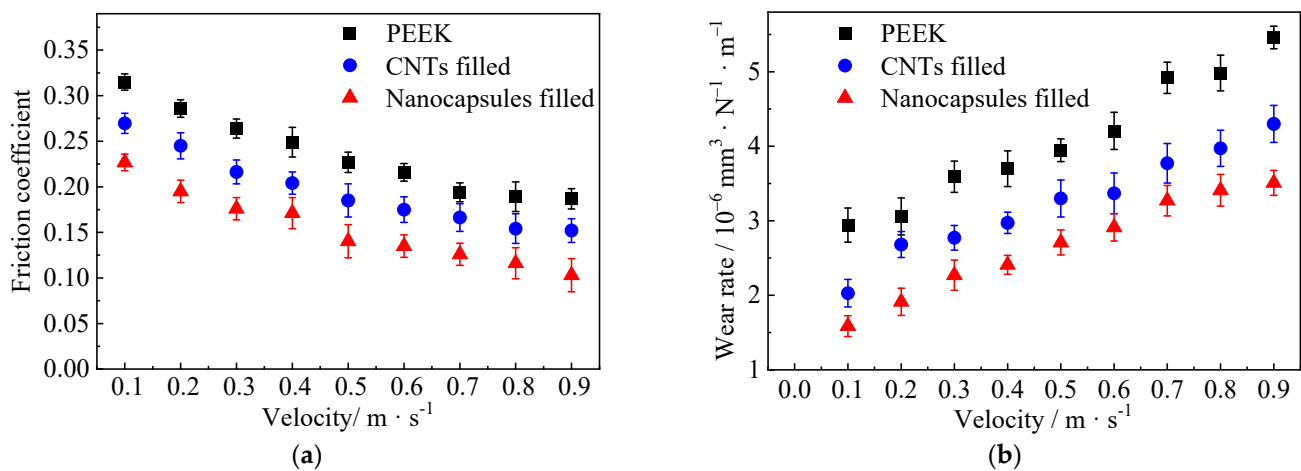


Figure 8. Influence of sliding speed on friction coefficient (a) and wear rate (b) of PEEK composites.

3.5. Effect of Test Load on Tribological Properties of PEEK Composites

Figure 9 shows the variation of the COF and WR of the three materials with the test load when the test sliding speed was 0.5 m/s. The coefficient of friction of the pure PEEK or PEEK/CNT composites gradually increases in Figure 9a for increasing loads that lead to larger frictional contact areas and heat generation [48]. However, the COF of the PEEK/nano-capsule composite did not change much or even decreased as a more sufficient lubrication layer was formed with the releasing of more RC2540. The PEEK/CNT composite had a smaller COF than ordinary PEEK under various loads. In Figure 9b, the WR of the three kind materials elevated with the TL, and the WR of the nano-capsule composite is the smallest. This may be due to the fact that at higher loads, more lubricating layers will be formed as the RC2540 is released.

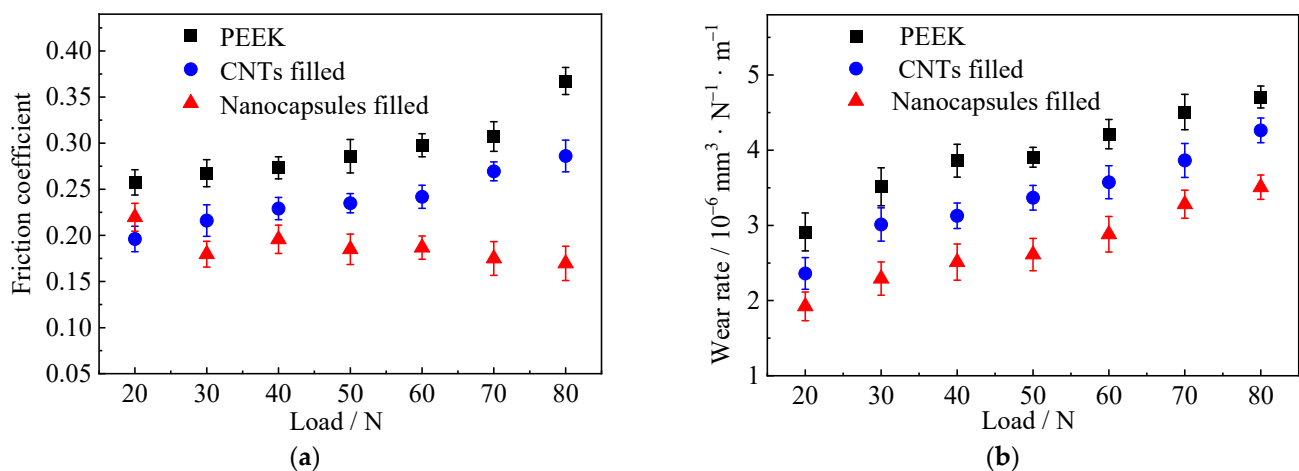


Figure 9. Influence of test load on PEEK composites' tribological properties of friction coefficient (a) and wear rate (b).

4. Discussion of Self-Lubrication Mechanism Analysis of PEEK Composite

4.1. SEM Analysis of the Worn Surface on Steel Disc

SEM morphology regarding the worn surface on steel disc and EDS energy spectrum of selected areas under the friction of the pure PEEK, PEEK/CNT composite and PEEK/nano-capsule composites are indicated in Figure 10. In Figure 10(a1–c1), the steel disc wear surface has deeper furrows in the presence of pure PEEK, better surface quality in the presence of the PEEK/CNT composite and the smoothest wear surface in the presence of the PEEK/nano-capsules. In addition, the worn surface under the action of pure PEEK has

more adhesions that are transfer films formed by PEEK. The adhesion of the CNT/PEEK composite or PEEK/nano-capsule composite is relatively low. The involvement of CNTs in the friction process is capable of reducing the PEEK adhesion and improving the surface quality of worn surface, while the release of RC2540 from the nano-capsules further reduces the adhesion of PEEK, and a lubricating layer may have some polishing effect, which may also improve the surface quality [49]. Figure 10(a2–c2) suggest that the worn surface under PEEK friction has a high elemental content of C and Fe, which is mainly a result of the transfer of PEEK materials to the metal surface. When CNTs or nano-capsules are involved in the friction process, the content of C increases and that of Fe decreases. This suggests that CNTs are decomposed and deposited on the metal surface for creating a lubrication layer during the friction process, and RC2540 can be released to the friction surface during the action of nano-capsules. The releasing and adsorption of RC2540 further increases the content of C and forms a more adequate lubrication layer, resulting in the reduced adhesion of PEEK. As shown in Figure 10(c2), the release of RC2540 is well demonstrated by the significant increase in elemental S content on the wear surface in the presence of the PEEK/nano-capsule composite.

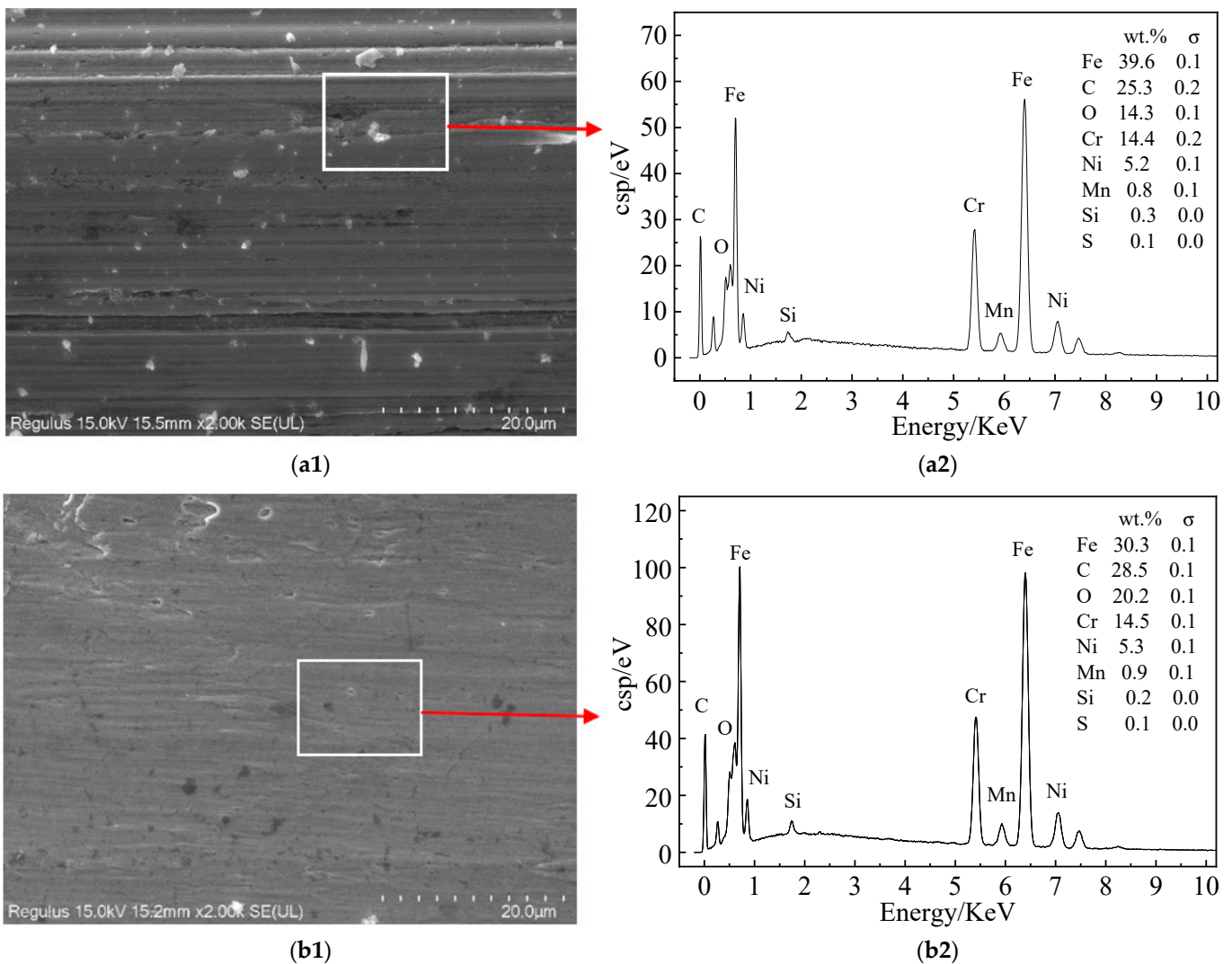


Figure 10. Cont.

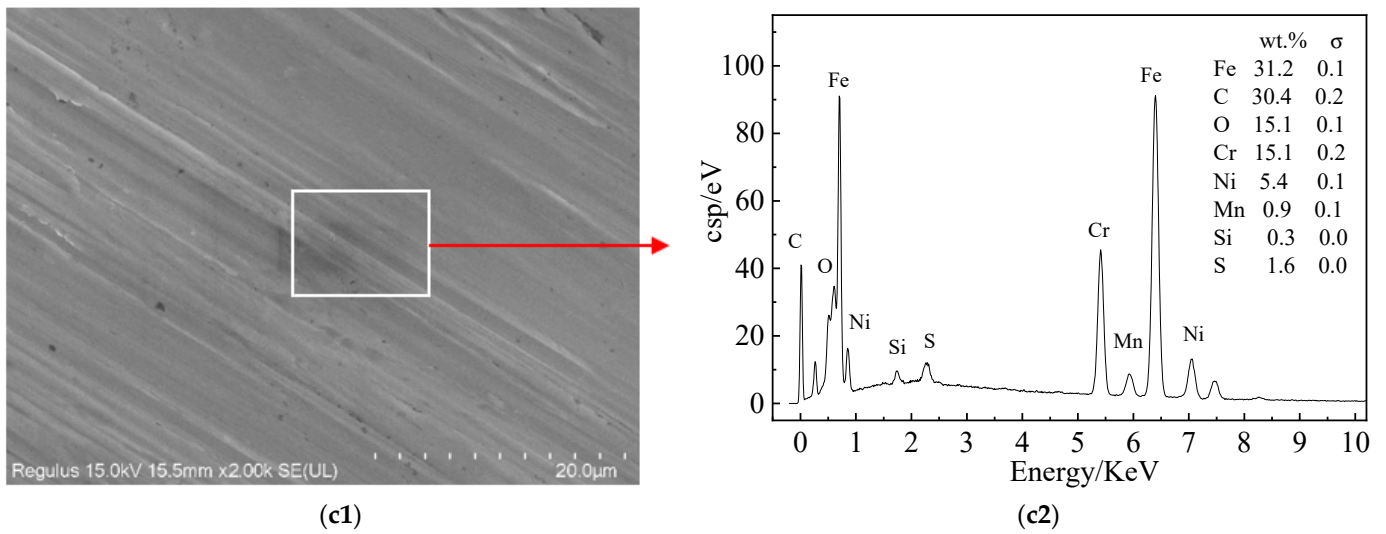


Figure 10. SEM surface morphology and EDS energy spectrum of worn surface of GCr15 steel under the action of pure PEEK (a1,a2), PEEK/CNT composites (b1,b2), PEEK/nano-capsule composites (c1,c2).

4.2. XPS Analysis of Worn Surface on Steel Disc

To further confirm the composition of the self-lubricating layer formed by CNTs@RC2540 nano-capsules, XPS energy spectrum analysis was conducted on the steel disc worn surface (Figure 11). XPSPEAK 41 software is applied to separate peaks of C, O and S. The obtained fitted peaks together with their possible corresponding functional groups are marked in the figure. Table 2 presents the relative atomic concentrations of elements on the worn surface.

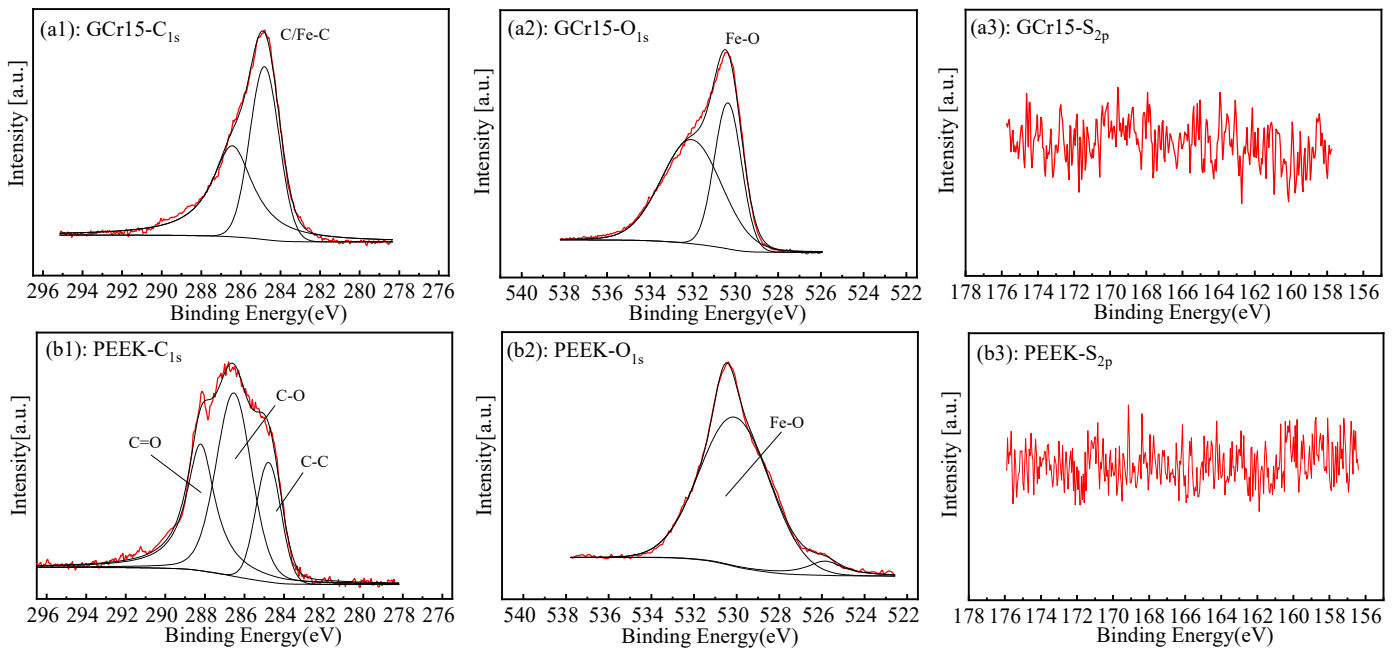


Figure 11. Cont.

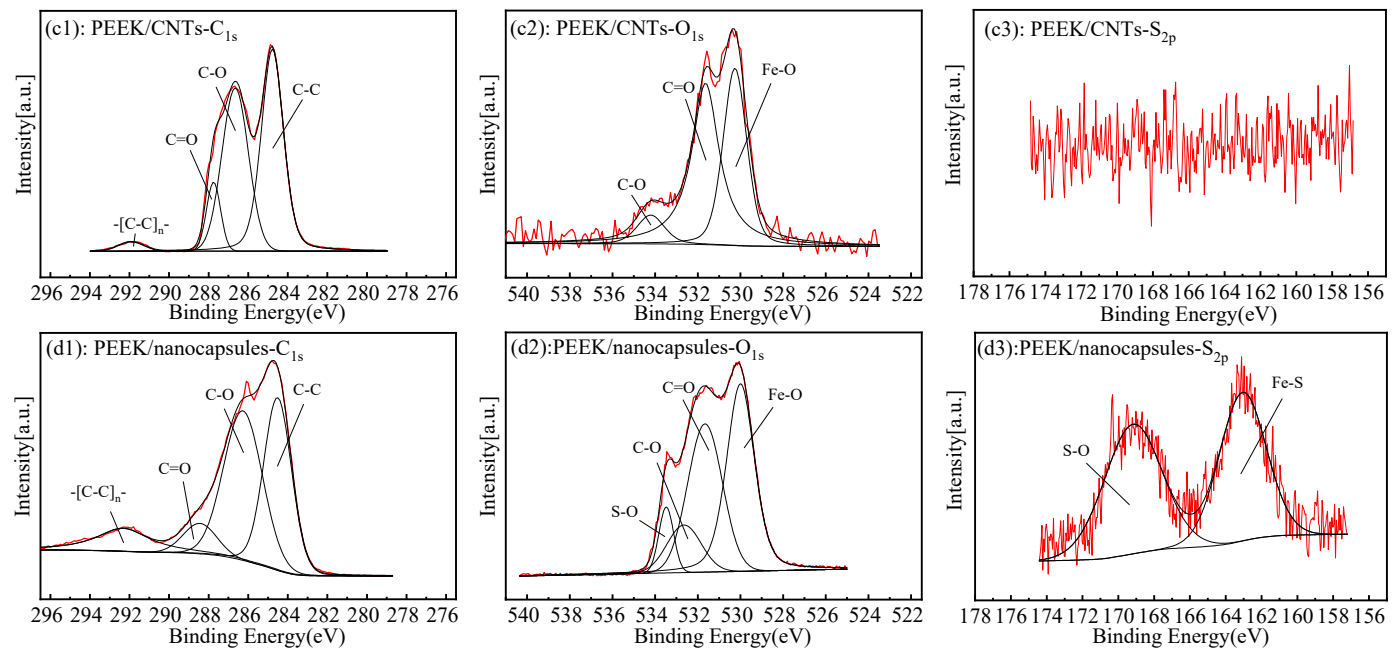


Figure 11. XPS energy spectra of C, O, and S on GCr15 steel surface (a1–a3) and the GCr15 worn surface under the friction of PEEK (b1–b3), PEEK/CNT composite (c1–c3), PEEK/nano-capsule composite (d1–d3).

Table 2. Relative atomic content of main elements on GCr15 steel and worn surface under the friction of different materials.

Type of Steel Surfaces under Test	Relative Content/%			
	C	O	Fe	S
Pure GCr15 steel	25.54	29.58	44.83	0.05
Under friction of PEEK	35.36	26.27	38.29	0.08
Under friction of PEEK/CNT composites	38.34	28.36	33.24	0.06
Under friction of PEEK/nano-capsule composites	30.95	32.41	34.53	2.11

The C and O spectra of the GCr15 steel surface in Figure 11(a1,a2) have a single peak shape, which mainly marks the oxygen in polluting carbon and iron oxides. The steel disc wear surface under pure PEEK friction has two new peaks in the C and O spectra compared to the GCr15 steel surface, which may be a result of the adhesive segments of PEEK. In Table 2, the adhesion of PEEK fragments is demonstrated by the increased atomic concentrations of C and the decreased atomic concentrations of O on the wear surface under friction with pure PEEK as compared to the surface of GCr15 steel. Such adhesion mainly depends on Van der Waals' force, hydrogen bond force and electrostatic force, which cause the PEEK fragments to bond chemically to the iron atoms, consequently reducing the atomic concentrations of O [50–52].

The peak shape for the C element of the worn surface rubbed by PEEK/CNT composite is similar to that of pure PEEK, and the fitting peak is primarily resulted from the carbon types in C-C, C-O and C=O in Figure 11(c1,c2) [53–56]. In Table 2, the highest atomic concentrations of C can be observed when the PEEK/CNT composites were rubbed, which suggests that the friction products of CNTs are adsorbed and deposited in the friction process. The PEEK/CNT-composite-forming lubrication layer is different from that formed by pure PEEK. In the friction process, the molecular structure of CNTs is destroyed, with some of the carbonized fragments deposited on or absorbed into the worn surface for weakening the friction.

In Figure 11(d3), the worn surface under action of the PEEK/nano-capsule composite has a distinct peak shape of S element, which appears at 161.2 eV and 168.3 eV,

respectively. The two peaks may be attributed to the sulfur species in Fe-S and S-O, respectively [57–59], which is good evidence for the release of RC2540 lubricant during friction. In Figure 11(d1,d2), the peak shape of C on the worn surface under friction of the PEEK/nano-capsule composite is similar to that of the PEEK/CNT composite. The fitting peak belonging to C-O has a stronger strength, and the peak shape of O element is more complex. These results indicate that CNTs in nano-capsules affect the friction, while the releasing of RC2540 in the nano-capsules impacts the formation of the lubricating layer of CNTs at the same time. Table 2 shows that the PEEK/nano-capsule composite has the lowest atomic concentration of C and the highest atomic concentration of O, while there is an intermediate concentration of Fe among the three kinds of worn surfaces. During frictions, RC2540 was released from the composite. The S element in the RC2540 molecule is highly reactive and readily binds to iron atoms through chemical adsorption, resulting in increased atomic concentrations of O and Fe elements and decreased atomic concentrations of C elements.

4.3. SEM Analysis of Worn Surface on Composites

Figure 12 gives the SEM analysis results of the worn surface of PEEK, the PEEK/CNT composite, and the PEEK/nano-capsule composite at a test load of 50 N, a sliding speed of 0.5 m/s and a filler content of 5%. With adhesion on the surface of friction pair and cyclic alternating shear stress on PEEK surface, the pure PEEK material wears mainly as a secondary surface fatigue spalling wear [60]. In addition, the surface material of PEEK can easily undergo thermoplastic deformation and flow under the action of friction temperature and stress, as shown in Figure 12a, as a result, the COF and the WR of pure PEEK materials are higher [61].

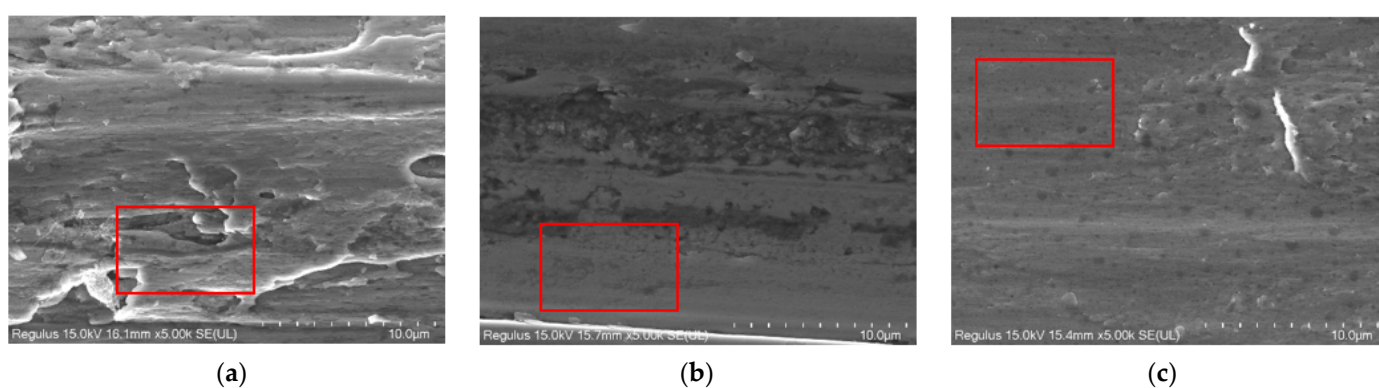


Figure 12. SEM micrographs of worn surfaces of PEEK (a), PEEK/CNT composite (b) and PEEK/nano-capsule composite (c).

In Figure 12b, the PEEK/CNT composites' worn surface shows no thermoplastic deformation and flow onto the material surface caused by friction temperature and stress, mainly as a result of the improved flexural strength, modulus and hardness of the PEEK composite as well as the load-bearing capacity of the CNTs. On the other hand, CNTs are directly involved in friction and also act as a lubricant. CNTs partially replace the direct contact between the matrix PEEK and GCr15 steel, reducing the real contact area between the resin and GCr15 steel, and effectively lowers the adhesion between the resin and the steel surface. The lubricating layer formed by CNTs also reduces the abrasive wear effect during the friction process and inhibits PEEK composites' thermoplastic deformation and wear, so that the wear resistance can be improved. However, the lubrication layer formed by CNTs only has a limited lubrication effect on the wearing surface, as the CNTs molecules do not have effective lubricating groups. The poor anti-friction and anti-wear effect of PEEK/CNTs resulted in the deep furrows on the worn surface.

The wear surface of the PEEK/nano-capsule composite also shows no significant plastic deformation or flow, as shown in Figure 12c, and the surface is much smoother. In

the friction process, the CNTs of the nano-capsules shell can first act as a friction reducer, and then the RC2540 in the nano-capsules can also be released to form a more sufficient lubricating layer, providing better friction and wear reduction, so the PEEK/nano-capsule composite exhibits the best tribological properties. Figure 13 gives the friction contact area model when applying PEEK/nano-capsules. The friction process is accompanied by the release of RC2540 from the nano-capsules, acting together with the friction products of CNTs for the formation of a more sufficient self-lubrication layer. RC2540 can also strengthen chemisorption, and the self-lubricating layer formed by it possesses three functions: First, the COF between PEEK and steel is reduced. Second, the WR is lowered. Third, the worn surface quality of PEEK composites and the steel disc are improved.

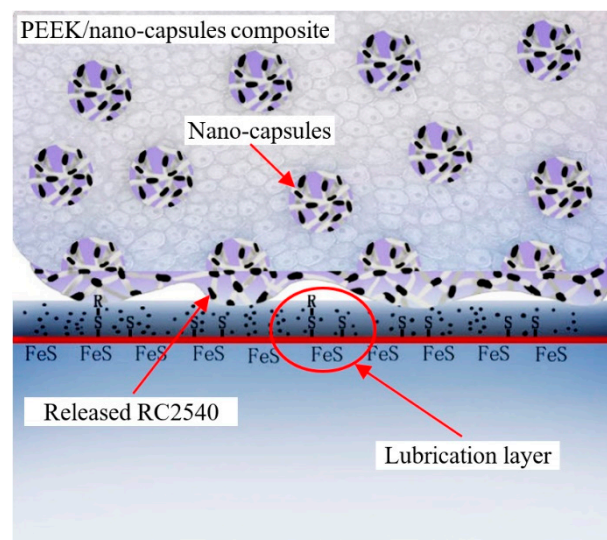


Figure 13. The model of self-lubrication layer under the friction of PEEK/nano-capsule composites.

5. Conclusions

Compared to the previous methods of adding CNTs for reinforcement in previous publications, the method of adding CNTs@RC2540 composites in this article can better increase the mechanical strength of PEEK materials and make it have better self-lubricating properties, which have broader application potential. The conclusions of this article are as follows:

- (a) This study demonstrated the successful preparation of CNTs@RC2540 nano-capsules whose filling rate reached approximately 25% TG, and DSC analysis proved the thermal stability of the composites. The nano-capsules completely resist the curing temperature of PEEK with their intact structure during curing. PEEK tissue exists in the form of cluster particles, which forms a good protection for RC2540.
- (b) After filling with nano-capsules, the tensile strength and hardness of PEEK are changed, but the actual mechanical property conditions of the self-lubricating parts can still be met within a certain filling range.
- (c) The filling of nano-capsules can significantly reduce the COF and WR of PEEK. Within a certain range, the higher the filling amount, the more significant the improvement in the COF. With the increase in experimental speed and loading, the COF of PEEK/nano-capsule composites also decreases, while the WR increases.
- (d) PEEK composite material filled with CNTs@RC2540 nano-capsules can release RC2540 during friction, which is adsorbed on the worn surface and acts with CNTs for forming a self-lubrication layer. The surface layer of the contact area from the combined action of the two components acts as a friction reduction, anti-wear and the surface quality improvement.

Author Contributions: J.G.: Writing—review and editing, supervision, resources, writing—original draft, formal analysis, conceptualization, data curation. Z.X.: Writing—review and editing, writing—original draft, investigation, formal analysis, conceptualization, data curation. L.Z.: Writing—review

and editing, funding acquisition, conceptualization, data curation. L.Y.: Conceptualization, data curation. J.G. and S.H.: Resources, formal analysis, Conceptualization, data curation. All authors have read and agreed to the published version of the manuscript.

Funding: Funding was provided by National Natural Science Foundation of China (51805345 and 52275468).

Data Availability Statement: Data are contained within the article.

Conflicts of Interest: The authors declare no conflict of interest.

References

1. Shang, Y.; Wu, X.; Liu, Y.; Jiang, Z.; Zhang, H. Preparation of PEEK/MWCNTs composites with excellent mechanical and tribological properties. *High Perform. Polym.* **2018**, *31*, 095400831775072. [[CrossRef](#)]
2. Yan, M.; Tian, X.; Yao, R. Processability and reusability of CF/PEEK mixture for Powder Bed Fusion of high strength composites. *Compost. Commun.* **2022**, *35*, 101318. [[CrossRef](#)]
3. Wang, Y.; Shen, J.; Yan, M.; Tian, X. Poly ether ether ketone and its composite powder prepared by thermally induced phase separation for high temperature selective laser sintering. *Mater. Des.* **2021**, *201*, 109510. [[CrossRef](#)]
4. Jean-Fulcrand, A.; Masen, M.A.; Bremner, T.; Wong, J.S.S. Effect of temperature on tribological performance of polyetheretherketone-polybenzimidazole blend-ScienceDirect. *Tribol. Int.* **2019**, *129*, 5–15. [[CrossRef](#)]
5. Zhang, L.; Li, G.; Guo, Y.; Qi, H.; Che, Q.; Zhang, G. PEEK reinforced with low-loading 2D graphitic carbon nitride nanosheets: High wear resistance under harsh lubrication conditions. *Compos. Part A Appl. Sci. Manuf.* **2018**, *109*, 507–516. [[CrossRef](#)]
6. Zhang, L.; Qi, H.; Li, G.; Wang, D.; Wang, T.; Wang, Q.; Zhang, G. Significantly enhanced wear resistance of PEEK by simply filling with modified graphitic carbon nitride. *Mater. Des.* **2017**, *129*, 192–200. [[CrossRef](#)]
7. Qin, Y.; Peng, Q.; Zhu, Y.; Zhao, X.; Lin, Z.; He, X.; Li, Y. Lightweight, mechanically flexible and thermally superinsulating rGO/polyimide nanocomposite foam with an anisotropic microstructure. *Nanoscale Adv.* **2019**, *1*, 4895–4903. [[CrossRef](#)] [[PubMed](#)]
8. Zalaznik, M.; Novak, S.; Huskić, M.; Kalin, M. Tribological behaviour of a PEEK polymer containing solid MoS₂ lubricants. *Lubr. Sci.* **2016**, *28*, 27–42. [[CrossRef](#)]
9. Moskalewicz, T.; Kruk, A.; Sitarz, M.; Kopia, A. Effect of the Processing and Heat Treatment Route on the Microstructure of MoS₂/Polyetheretherketone Coatings Obtained by Electrophoretic Deposition. *J. Electrochem. Soc.* **2019**, *166*, D151–D161. [[CrossRef](#)]
10. Ata, S.; Hayashi, Y.; Nguyen Thi, T.B.; Tomonoh, S.; Kawauchi, S.; Yamada, T.; Hata, K. Improving thermal durability and mechanical properties of poly(ether ether ketone) with single-walled carbon nanotubes. *Polymer* **2019**, *176*, 60–65. [[CrossRef](#)]
11. Su, Y.; Zhang, S.; Zhang, X.; Zhao, Z.; Jing, D. Preparation and properties of carbon nanotubes/carbon fiber/poly(ether ether ketone) multiscale composites. *Compos. Part A Appl. Sci. Manuf.* **2018**, *108*, 89–98. [[CrossRef](#)]
12. Rashidi, E.; Rezaie, H.; Ghassai, H. The effect of carbon nanotube addition on the mechanical properties and biological functionality of poly-ether-ether-ketone-hydroxyapatite composites. *Polym. Compos.* **2021**, *42*, 3253–3261. [[CrossRef](#)]
13. Kalin, M.; Zalaznik, M.; Novak, S. Wear and friction behaviour of poly-ether-ether-ketone (PEEK) filled with graphene, WS₂ and CNT nanoparticles. *Wear* **2015**, *332–333*, 855–862. [[CrossRef](#)]
14. Song, H.; Li, N.; Li, Y.; Min, C.; Wang, Z. Preparation and tribological properties of graphene/poly(ether ether ketone) nanocomposites. *J. Mater. Sci.* **2012**, *47*, 6436–6443. [[CrossRef](#)]
15. Poudel, Y.R.; Li, W. Synthesis, properties, and applications of carbon nanotubes filled with foreign materials: A review. *Mater. Today Phys.* **2018**, *7*, 7–34. [[CrossRef](#)]
16. Shi, L.; He, Y.; Hu, Y.; Wang, X. Controllable natural convection in a rectangular enclosure filled with Fe₃O₄@CNT nanofluids. *Int. J. Heat Mass Transf.* **2019**, *140*, 399–409. [[CrossRef](#)]
17. Wang, W.; Lin, L.; Yu, D.; Liu, B. Study on the Photocatalytic Performance of BiVO₄/Bi₂WO₆/Multi-Walled Carbon Nanotube Nanocomposites in One-Pot Hydrothermal Process. *J. Nanosci. Nanotechnol.* **2018**, *18*, 7691–7702. [[CrossRef](#)]
18. Qu, S.; Yao, P.; Gong, Y.; Chu, D.; Yang, Y.; Li, C.; Wang, Z.; Zhang, X.; Hou, Y. Environmentally friendly grinding of C/SiCs using carbon nanofluid minimum quantity lubrication technology. *J. Clean. Prod.* **2022**, *366*, 132898. [[CrossRef](#)]
19. Zheng, G.; Zhang, S.; Chu, W.; Luo, J.; Zuo, X. Heterocoagulation method for preparation of composite fluoropolymer particles with core-shell structure for optimized electromagnetic performance. *J. Mater. Sci. Mater. Electron.* **2021**, *32*, 3116–3124. [[CrossRef](#)]
20. Wang, Y.; Guan, J.; Wang, J.; Feng, B.; Xu, X. Electrical Conductivity and Wettability of Nanofluids Prepared by Nanocomposite of MWCNTs and Dialkyl Pentasulfide. *Curr. Nanosci.* **2021**, *17*, 151–161. [[CrossRef](#)]
21. Yang, H.; Li, B.; Cui, R.; Xing, R.; Liu, S. Electrochemical sensor for rutin detection based on Au nanoparticle-loaded helical carbon nanotubes. *J. Nanoparticle Res.* **2017**, *19*, 354. [[CrossRef](#)]
22. Zhai, M.; Cui, R.; Gu, N.; Zhang, G.; Lin, W.; Yu, L. Nanocomposite of Au Nanoparticles/Helical Carbon Nanofibers and Application in Hydrogen Peroxide Biosensor. *J. Nanosci. Nanotechnol.* **2015**, *15*, 4682–4687. [[CrossRef](#)]
23. Zuo, M.; Yuan, X.; Wang, S.; Zhu, W.; Zuo, X.; Geng, F. Solventless preparation of ammonium persulfate microcapsules with a polypyrrole shell. *J. Mater. Sci.* **2018**, *54*, 5898–5906. [[CrossRef](#)]

24. Song, Y.; Wang, Z.; Zhang, X.; Zhang, R.; Li, J. Synthetic Process of Bio-Based Phenol Formaldehyde Adhesive Derived from Demethylated Wheat Straw Alkali Lignin and Its Curing Behavior. *J. Renew. Mater.* **2021**, *9*, 943–957. [[CrossRef](#)]
25. Yu, X.; Zhang, B.; Gu, B. Creep and Stress Relaxation Performance of Rubber Matrix Sealing Composites after Fatigue Loading. *Fibers Polym.* **2021**, *23*, 471–477. [[CrossRef](#)]
26. Yu, X.; Zhang, B.; Gu, B. Fatigue Behavior of Aramid Fiber Reinforced Rubber Matrix Sealing Composites. *Fibers Polym.* **2021**, *22*, 1111–1119. [[CrossRef](#)]
27. Zuo, M.; Zhang, Q.; Mei, H.; Zhang, J.; Zuo, X.; Geng, F. Preparation and characterization of polymer microcapsules containing ammonium persulfate with controlled burst release. *Mater. Res. Express* **2019**, *6*, 105332. [[CrossRef](#)]
28. Dumas, J.P.; Gibout, S.; Cézac, P.; Franquet, E. New theoretical determination of latent heats from DSC curves. *Thermochim. Acta* **2018**, *670*, 92–106. [[CrossRef](#)]
29. Zhang, C.; Wang, D.; Qian, S.; Zhang, Z.; Liang, X.; Wu, L.; Long, L.; Shi, H.; Han, Z. Giant barocaloric effects with a wide refrigeration temperature range in ethylene vinyl acetate copolymers. *Mater. Horiz.* **2022**, *9*, 1293–1298. [[CrossRef](#)] [[PubMed](#)]
30. Wang, S.; Zhang, W.; Chen, Y.; Zhang, S.; Wang, W. The Aromatic Properties of Polyurea-Encapsulated Lavender Oil Microcapsule and Their Application in Cotton Fabrics. *J. Nanosci. Nanotechnol.* **2019**, *19*, 4147–4153. [[CrossRef](#)]
31. Wang, S.J.; Zhu, W.X.; Liao, D.W.; Ng, C.F.; Au, C.T. In situ FTIR studies of NO reduction over carbon nanotubes (CNTs) and 1 wt.% Pd/CNTs. *Catal. Today* **2004**, *93–95*, 711–714. [[CrossRef](#)]
32. Bahrami Eynolghasi, M.; Mohammadi, T.; Tofighy, M.A. Fabrication of polystyrene (PS)/cyclohexanol-based carbon nanotubes (CNTs) mixed matrix membranes for vacuum membrane distillation application. *J. Environ. Chem. Eng.* **2022**, *10*, 108175. [[CrossRef](#)]
33. Wang, K.; Dong, H.; Zhou, D.; Ito, Y.; Hu, L.; Zhang, Z.; Zhu, X. Facile Fabrication of Semiconducting Single-Walled Carbon Nanotubes Patterns on Flexible Substrate Based on a Photoimmobilization Technique. *ACS Appl. Mater. Interfaces* **2020**, *12*, 8722–8729. [[CrossRef](#)] [[PubMed](#)]
34. Yang, L.; Liu, H.; Zhang, Y. Study on the tensile creep behavior of carbon nanotubes-reinforced Sn-58Bi solder joints. *J. Electron. Mater.* **2017**, *47*, 662–671. [[CrossRef](#)]
35. Zhu, S.; Qian, Y.; Hassan, E.A.M.; Shi, R.; Yang, L.; Cao, H.; Zhou, J.; Ge, D.; Yu, M. Enhanced interfacial interactions by PEEK-grafting and coupling of acylated CNT for GF/PEEK composites. *Compos. Commun.* **2020**, *18*, 43–48. [[CrossRef](#)]
36. Qian, D.; Dickey, E.C.; Andrews, R.; Rantell, T. Load transfer and deformation mechanisms in carbon nanotube-polystyrene composites. *Appl. Phys. Lett.* **2000**, *76*, 2868–2870. [[CrossRef](#)]
37. Ye, H.; Park, E.; Shin, S.C.; Murali, G.; Kim, D.; Lee, J.; Kim, I.H.; Kim, S.J.; Kim, S.H.; Jeong, Y.J.; et al. Photopatternable High-k Polysilsesquioxane Dielectrics for Organic Integrated Devices: Effects of UV Curing on Chemical and Electrical Properties. *Adv. Funct. Mater.* **2023**, *33*, 2214865. [[CrossRef](#)]
38. Zhang, B.; Yu, X.; Gu, B. An Improved Shear Lag Model for Predicting Stress Distribution in Hybrid Fiber Reinforced Rubber Composites. *Fibers Polym.* **2017**, *18*, 349–356. [[CrossRef](#)]
39. Khudaish, E.A.; Al-Badri, A. A modified Hummers soft oxidative method for functionalization of CNTs: Preparation, characterization and potential application for selective determination of norepinephrine. *Synth. Met.* **2021**, *277*, 116803. [[CrossRef](#)]
40. Kong, F.; Tao, S.; Qian, B.; Gao, L. Multiwalled carbon nanotube-modified Nb₂O₅ with enhanced electrochemical performance for lithium-ion batteries. *Ceram. Int.* **2018**, *44*, 23226–23231. [[CrossRef](#)]
41. Yin, X.; Wu, J.; Li, C.; Lu, X.; Feng, X.; Shi, Y. Right Way of Using Graphene Oxide Additives for Water-Lubricated PEEK: Adding in Polymer or Water? *Tribol. Lett.* **2018**, *66*, 103. [[CrossRef](#)]
42. Fan, F.X.; Zheng, Y.M.; Ba, M.; Wang, Y.F.; Kong, J.J.; Liu, J.H.; Wu, Q. Long time super-hydrophobic fouling release coating with the incorporation of lubricant. *Prog. Org. Coat.* **2021**, *152*, 106136. [[CrossRef](#)]
43. Dai, X.Z.; Guo, P.; Hong, D.M.; Hui, J.D.; Hui, Z.M.; Geng, F. The effect of preparation and characterisation of polyurea grease. *Mater. Res. Innov.* **2015**, *19*, S5-588–S5-591. [[CrossRef](#)]
44. Han, Y.; Liu, J.; Wang, Q.; Lin, C.; Wang, E.; Wu, W.; Zhang, M. Effect of volume fraction ratio of Ti to Al₃Ti on mechanical and tribological performances of the in situ Ti-Al₃Ti core-shell structured particle reinforced Al matrix composite. *J. Mater. Res.* **2022**, *37*, 3695–3707. [[CrossRef](#)]
45. Kucher, M.; Dannemann, M.; Füßel, R.; Weber, M.-T.; Modler, N. Sliding friction and wear of human teeth against biocompatible polyether ether ketone (PEEK) under various wear conditions. *Wear* **2021**, *486–487*, 204110. [[CrossRef](#)]
46. Tatsumi, G.; Ratoi, M.; Shitara, Y.; Sakamoto, K.; Mellor, B.G. Effect of organic friction modifiers on lubrication of PEEK-steel contact. *Tribol. Int.* **2020**, *151*, 106513. [[CrossRef](#)]
47. Lin, L.; Zhao, Y.; Hua, C.; Schlarb, A.K. Effects of the Velocity Sequences on the Friction and Wear Performance of PEEK-Based Materials. *Tribol. Lett.* **2021**, *69*, 68. [[CrossRef](#)]
48. Lin, L.; Pei, X.Q.; Bennewitz, R.; Schlarb, A.K. Tribological Response of PEEK to Temperature Induced by Frictional and External Heating. *Tribol. Lett.* **2019**, *67*, 52. [[CrossRef](#)]
49. Sun, Y.; Zhu, T.; Cai, M.; Zhang, Y.; Fan, C.; An, Z. Influence of grinding lubrication methods on surface integrity of nickel-based single crystal superalloy. *Diam. Abras. Eng.* **2022**, *42*, 201–207.
50. Puhan, D.; Wong, J.S.S. Properties of Polyetheretherketone (PEEK) transferred materials in a PEEK-steel contact. *Tribol. Int.* **2019**, *135*, 189–199. [[CrossRef](#)]

51. Song, J.; Liao, Z.; Shi, H.; Xiang, D.; Liu, Y.; Liu, W.; Peng, Z. Fretting Wear Study of PEEK-Based Composites for Bio-implant Application. *Tribol. Lett.* **2017**, *65*, 150. [[CrossRef](#)]
52. Ding, J.; Lu, Z.; Wu, M.; Liu, C.; Yang, Y.; Ji, H.; Yang, G. Carbon coated SnO₂ particles stabilized in the elastic network of carbon nanofibers and its improved electrochemical properties. *Mater. Chem. Phys.* **2018**, *215*, 285–292. [[CrossRef](#)]
53. Myshkin, N.K.; Petrokovets, M.I.; Kovalev, A.V. Tribology of polymers: Adhesion, friction, wear, and mass-transfer. *Tribol. Int.* **2005**, *38*, 910–921. [[CrossRef](#)]
54. Vishal, K.; Rajkumar, K. Dry sliding wear behavior of Poly Ether Ether Ketone (PEEK) reinforced with graphite and synthetic diamond particles. *Diam. Relat. Mater.* **2022**, *130*, 109404. [[CrossRef](#)]
55. Huang, Z.; Zhao, C.; Xu, R.; Zhou, Y.; Jia, R.; Xu, X.; Shi, S. Carbon modified hierarchical hollow tubes composed of TiO₂ nanoparticles for high performance lithium-ion batteries. *J. Alloys Compd.* **2021**, *857*, 158048. [[CrossRef](#)]
56. Ma, C.; Jiang, J.; Han, Y.; Gong, X.; Yang, Y.; Yang, G. The composite of carbon nanotube connecting SnO₂/reduced graphene clusters as highly reversible anode material for lithium-/sodium-ion batteries and full cell. *Compos. Part B Eng.* **2019**, *169*, 109–117. [[CrossRef](#)]
57. Qi, H.; Zhang, L.; Zhang, G.; Wang, T.; Wang, Q. Comparative study of tribochemistry of ultrahigh molecular weight polyethylene, polyphenylene sulfide and polyetherimide in tribo-composites. *J. Colloid Interface Sci.* **2018**, *514*, 615–624. [[CrossRef](#)]
58. Fan, X.; Hu, Y.; Zhang, Y.; Lu, J.; Chen, X.; Niu, J.; Li, N.; Chen, D. Reduced Graphene Oxide–Epoxy Grafted Poly(Styrene-Co-Acrylate) Composites for Corrosion Protection of Mild Steel. *Coatings* **2019**, *9*, 666. [[CrossRef](#)]
59. Wu, D.; Chen, Y.; Hong, X.; Wang, L.; Ou-Yang, W.; Tao, S.; Zhao, Q.; Qian, B.; Chu, P.K. Field emission from geometrically modulated tungsten-nickel sulfide/graphitic carbon nanobelts on Si microchannel plates. *Ceram. Int.* **2021**, *47*, 4034–4042. [[CrossRef](#)]
60. Pei, X.-Q.; Bennewitz, R.; Schlarb, A.K. Mechanisms of Friction and Wear Reduction by Carbon Fiber Reinforcement of PEEK. *Tribol. Lett.* **2015**, *58*, 42. [[CrossRef](#)]
61. Huang, J.; Wan, S.; Wang, L.; Xue, Q. Tribological Properties of Si-Doped Graphite-Like Amorphous Carbon Film of PEEK Rubbing with Different Counterparts in SBF Medium. *Tribol. Lett.* **2015**, *57*, 10. [[CrossRef](#)]

Disclaimer/Publisher’s Note: The statements, opinions and data contained in all publications are solely those of the individual author(s) and contributor(s) and not of MDPI and/or the editor(s). MDPI and/or the editor(s) disclaim responsibility for any injury to people or property resulting from any ideas, methods, instructions or products referred to in the content.